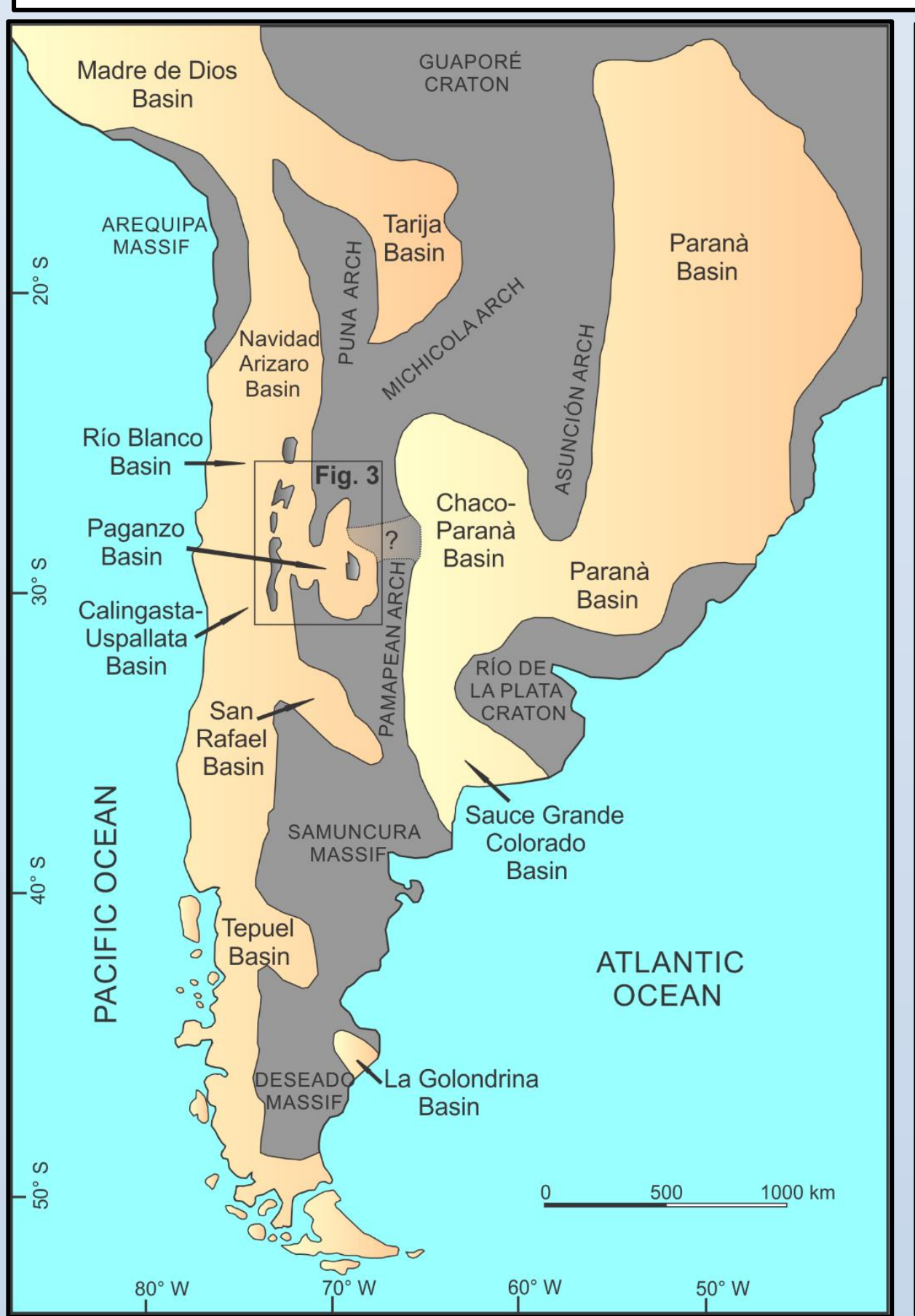


# DETRITAL ZIRCON GEOCHRONOLOGY AND SEDIMENTOLOGY OF GLACIOGENIC STRATA OF THE MIDDLE CARBONIFEROUS SAN EDUARDO FORMATION, CALINGASTA-USPALLATA BASIN, NW ARGENTINA

MALONE\*<sup>1</sup>, John E., ISBELL<sup>1</sup>, John L., BOWLES<sup>1</sup>, Julie A., PAGANI<sup>2</sup>, Alejandra M., TABOADA<sup>3</sup>, Arturo C., (1)Geosciences, University of Wisconsin-Milwaukee, Milwaukee, WI (2)Museo Paleontológico Egidio Ferugli, Trelew, Argentina (3)National University of Patagonia San Juan Bosco, Comodoro Rivadavia, Argentina

**ABSTRACT**  
The Calingasta-Uspallata Basin preserves a near continuous sequence of glaciomarine deposition from the middle to late Carboniferous, represented by five separate formations. Correlation between these formations has been achieved using index marine invertebrates, which also provides some implications for max-depositional ages. However, no isotopic dating analyses have been sought in this basin to further constrain the age of deposition or provide a source of provenance for sediments. The San Eduardo formation near the El Leoncito Astronomical Complex, San Juan Province, Argentina, was deposited within the Calingasta-Uspallata Basin on the western margin of the proto-Precordillera during the late Mississippian to early Pennsylvanian. This succession preserves a complete sequence of proximal glaciomarine, nearshore, and fluvial systems deposited at the beginning of the late Paleozoic ice age. Samples were collected from various stages throughout the sequence for detrital zircon U-Pb geochronology to determine sediment provenance as a way of isolating different glacial sources. Results indicate multiple stages of glaciation, with at least three distinct source areas. The lowermost stage includes locally sourced basement and recycled underlying Silurian, represented by similar Famatinian (500-460 Ma) and Sunsas peaks (1450-1000 Ma) peaks, with the Sunsas source likely originating from the Western Sierras Pampeanas, which would represent a breaching of the proto-Precordillera from the east. The middle stage shows a population distinct unto itself, with a peak during the Mississippian (330-360 Ma). A volcanic island arc was situated along the Andean margin during the late Paleozoic, likely resulting in the influx of Carboniferous aged volcanic sediments. The lower most stage shows relations based on K-S results to formations within the Paganzo basin to the northeast, likely serving as the outwash of these distant glaciers through braided fluvial systems. This study will expand upon current chronologic knowledge within the Calingasta-Uspallata basin and will be supported by sandstone petrology and mineralogic composition, pebble counts and composition of dropstones.



**BACKGROUND**  
Gondwana reached its maximum expansion during the Carboniferous-Permian transition, where in South America vast Upper Paleozoic basins along its southwestern margin constitute a link in the reconstruction of this paleocontinent history. These basins rest unconformably upon the Middle Devonian to earliest Mississippian fold-and-thrust belt, the proto-Precordillera, formed during the Chañi orogen as the Chileña terrane thrust and accreted to the western margin of Gondwana (Ramos et al., 1984, 1986). The Calingasta-Uspallata, Rio Blanco, and Paganzo foreland Basins formed synorogically and these basins are separated from those to the east by the Pampean arch. Post-collisional extension dominated during the Pennsylvanian as subduction shifted westward, which allowed these basins to widen into a back-arc setting (Limarino et al., 2006). The proto-Precordillera created a paleotopographic high, from which alpine glaciers extend both east and westward into the adjacent basins. The purpose of this research was to determine the detrital zircon provenance of several facies within the San Eduardo Formation within the Calingasta-Uspallata basin. These data will be compared to available data in the Paganzo, Paraná, and Colorado basins to determine the temporal and spatial contexts of sediment dispersal.

Figure 1. Regional location map of the distribution of late Paleozoic basins in South America. Modified from Henry et al. (2010).

**METHODOLOGY**  
A 700 m section San Eduardo Formation was measured and described in the exposed several km east of the Leoncito Observatory. Six samples were collected detrital zircon geochronology (n=1226 total zircons analyzed). The San Eduardo includes hemipelagic shale, debris flow deposits, as well as shallow marine and fluvial sandstone. No ice-contact or subglacial sediment was observed in this succession. Sampling horizons included the underlying Silurian strata (US1A 1902), three submarine channel sandstone beds within diamicton-bearing succession (SE1A 1901, SE1D 1905, SE1E 1907), and two from the overlying fluvial-marine transgressive succession (SE1F 1910, SE1F 1911). U-Pb geochronology of zircons was conducted by laser ablation inductively coupled plasma mass spectrometry (LA-ICPMS) at the Arizona LaserChron Center (Gehrels et al., 2008, 2014). The analyses involve ablation of zircon with a Photon Machines Analyte G2 excimer laser equipped with Helix ablation cell using a spot diameter of 20 microns. Following analysis, data reduction was performed with an in-house Python decoding routine and an Excel spreadsheet (E2agecalc). The ages are shown on relative age-probability diagrams using the routines in Isoplot (Ludwig, 2008). A K-S analysis was completed to compare the age spectra of the samples analyzed here with published data from Craddock et al. (2019).

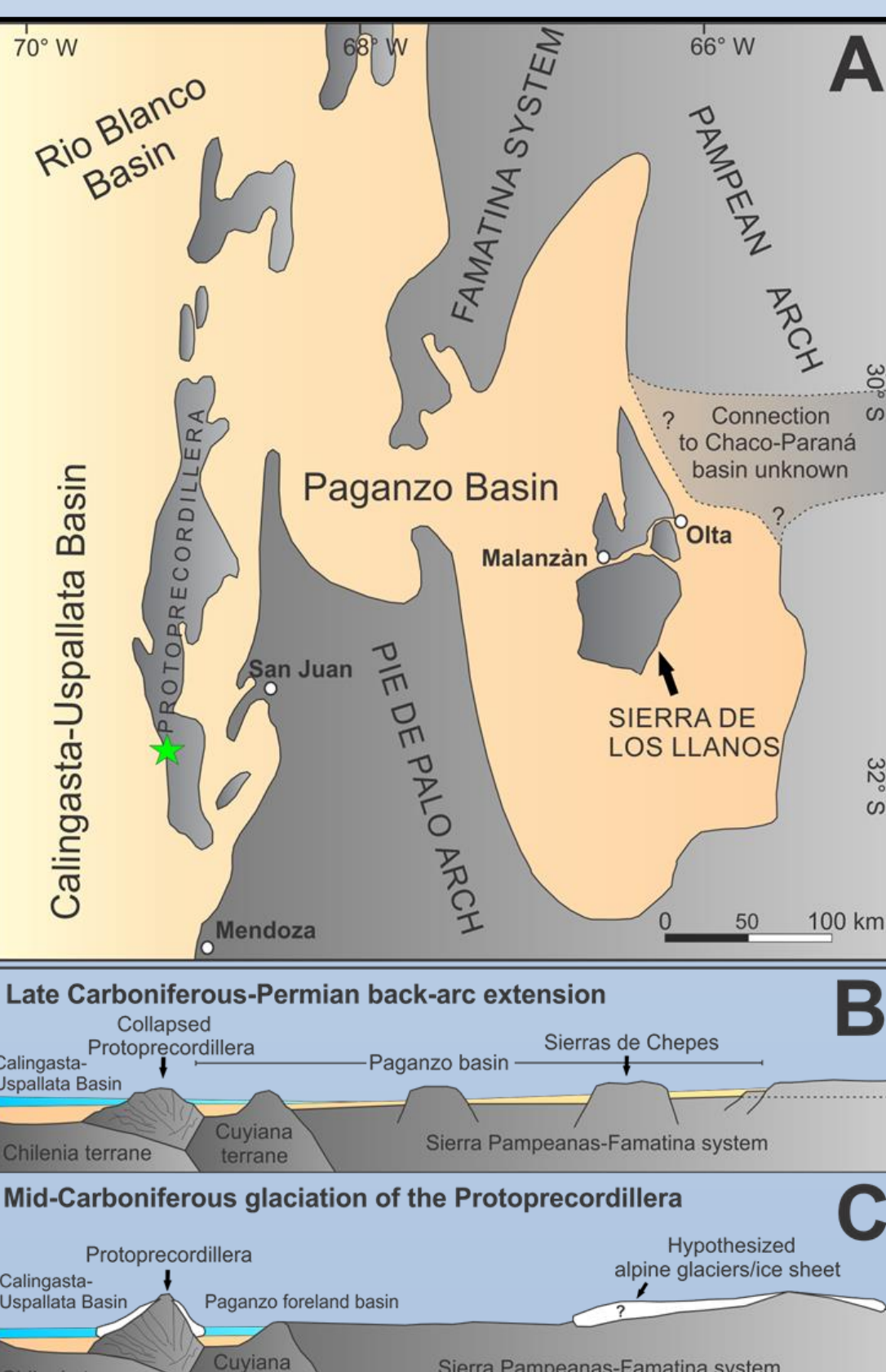


Figure 2. Tectonic setting of sedimentary basins and fold and thrust belts in northwest Argentina during the late Carboniferous-early Permian. Modified from Isbell et al. (2012). Green star = study area.

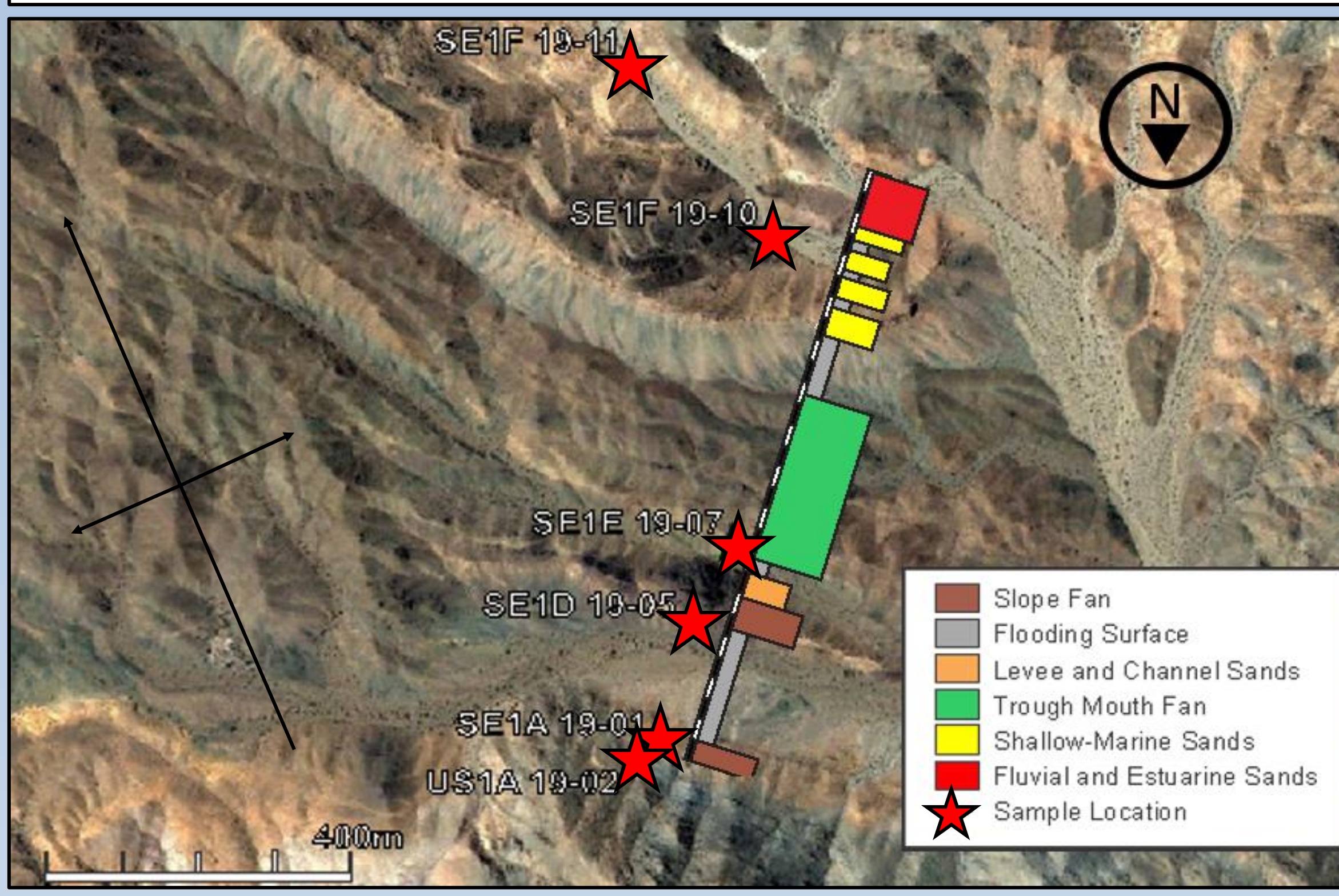


Figure 3. Map of study area showing the position of the measured section. Green stars = sampling.

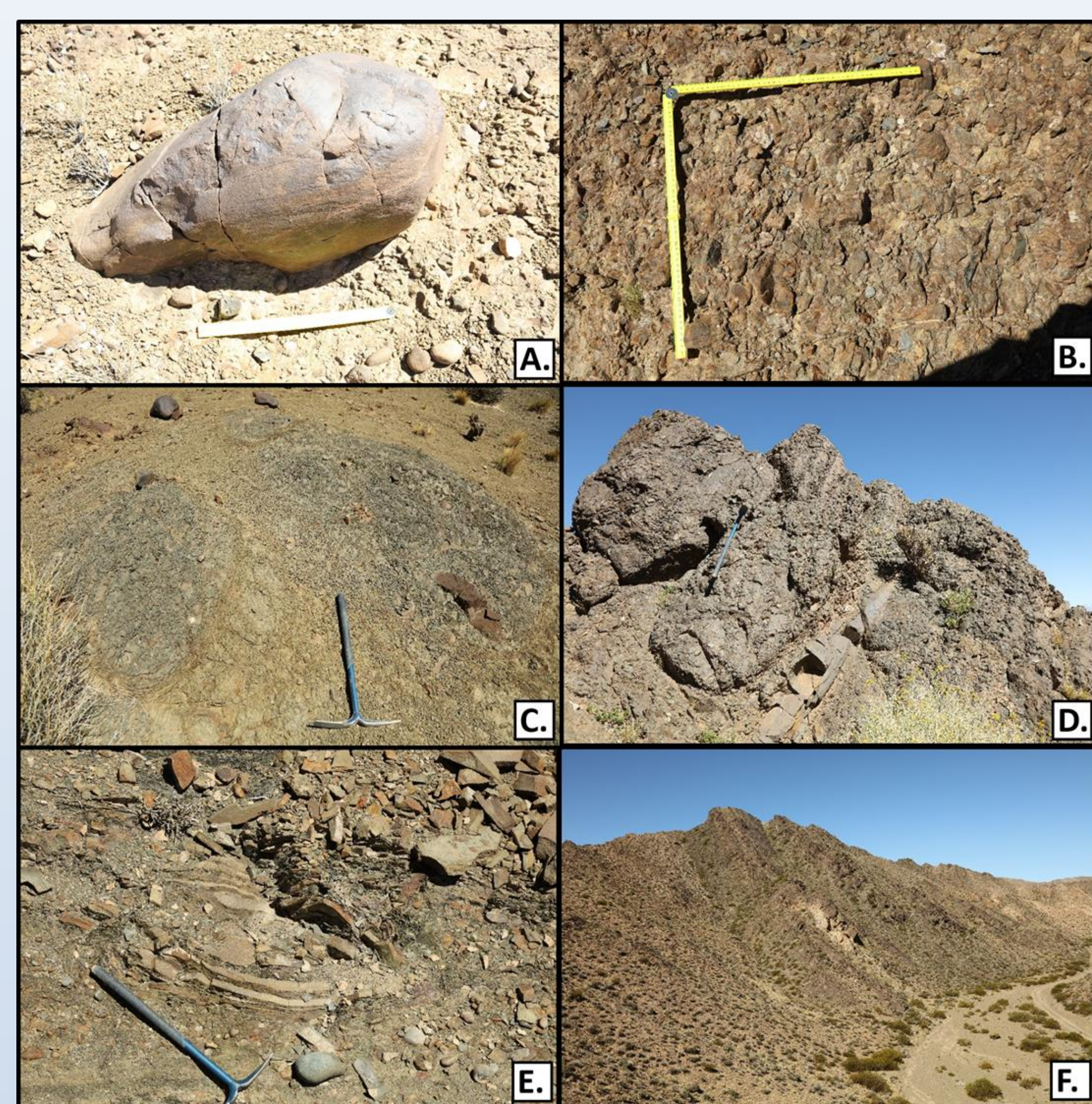


Figure 4. Photo mosaic of lithofacies and sedimentary structures present in the San Eduardo Formation. A. Faceted lithic wacke boulder in clast-supported sandy diamicton located near the top of the distal-glacial sequence, likely transported via ice rafting. B. Clast-supported sandy diamicton; the principle lithofacies comprising the trough mouth fan deposit. Pebble composition is predominately siliciclastic with occasional plutonic clasts. C. Clast-rich muddy diamicton surrounded by clast-poor thinly laminated to massive mudstones, interpreted to be an ice-rafted dump structure. D. Cross-bedding preserved in sandy diamicton. Sand layers wedge out and onlap onto adjacent diamictons, suggesting channel and levee topping deposition. E. Transverse view of a sheath fold located at the top of the distal-glacial sequence. The direction of slumping is along the z-axis. F. Stacked parasequences exposed near the top of the San Eduardo Formation. The parasequences thin in thickness with increasing elevation, suggesting a slowing down of relative sea level rise.

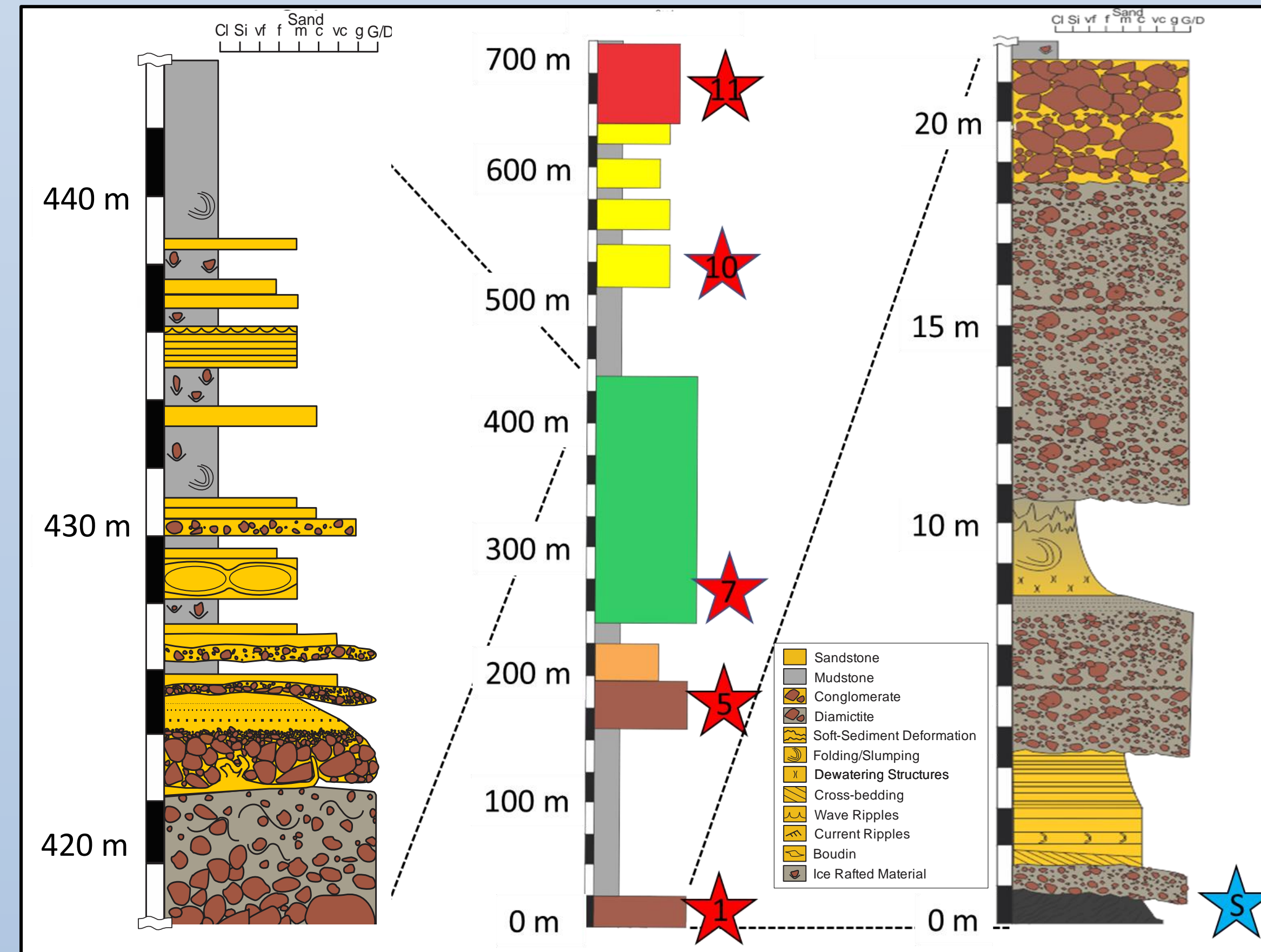


Figure 5. Drafted stratigraphic columns representing a slope-to-shelf transition. The column on the right is the basal member and is interpreted to represent a slope fan. The column on the left shows the shift from a trough mouth fan to a coarse-clastic starved depositional regime. Stars = sample location.

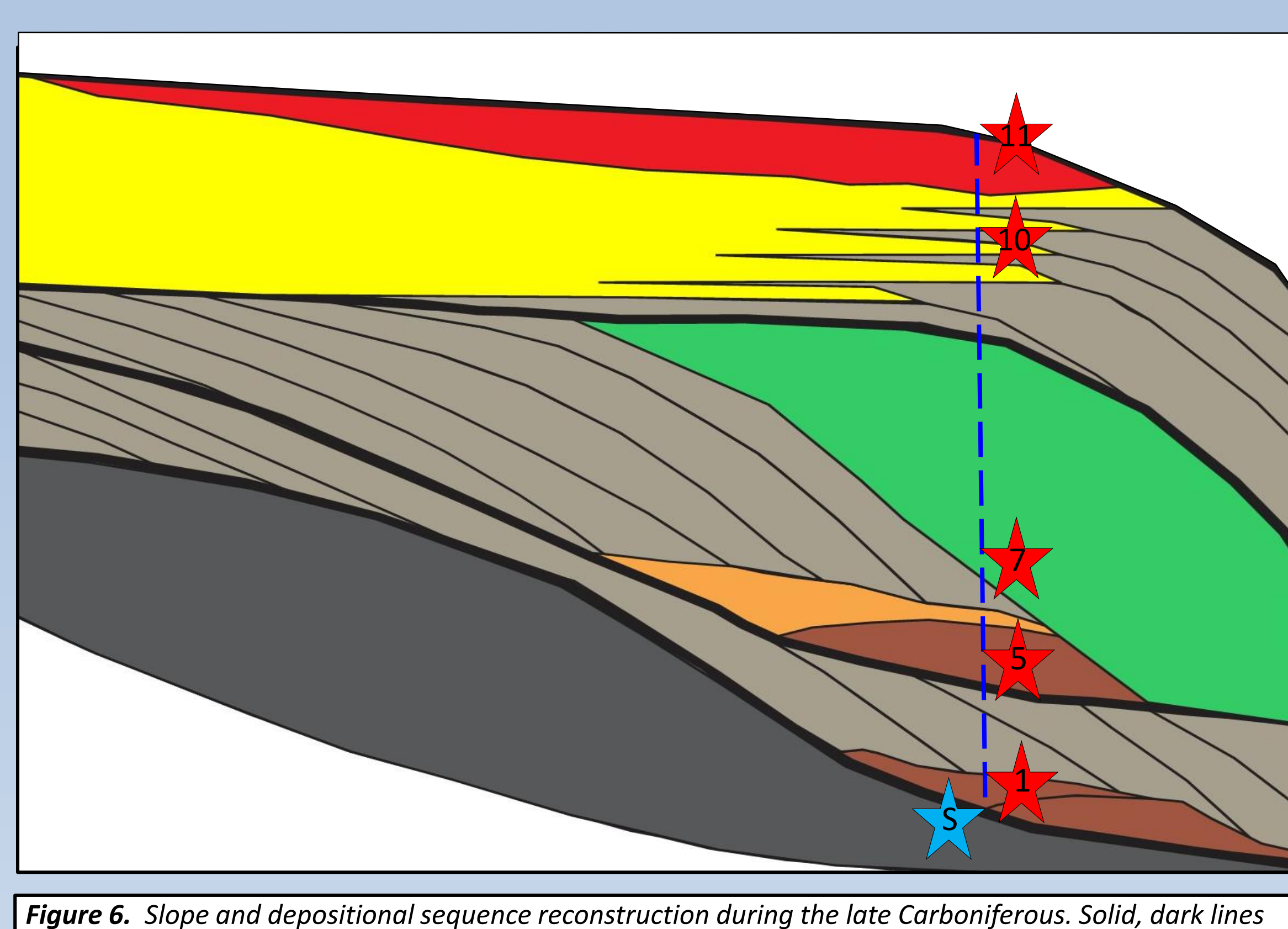


Figure 6. Slope and depositional sequence reconstruction during the late Carboniferous. Solid, dark lines represent sequence boundaries. The dashed blue line represents the measured transect.

**RESULTS**  
Sample US1A 1902 (n=211), which was taken from the underlying Silurian strata has zircons that range in age from 451-2794 Ma. The principal age peak is 1099 Ma with a lesser peak of 470 Ma. The age spectra for sample SE1A 1901 (n=101) ranges from 321-2043 Ma. Age peaks are 1170, 1078, 453 and 365 Ma. Sample SE1D 1905 (n=215) has age peaks of 364, 1102, and 1384 Ma and the age spectrum ranges from 321-2702 Ma. Sample SE1E 1907 (n=214) has a principal age peak of 366 Ma and a lesser peak at 1098 Ma. The detrital zircon age spectrum 330-2785 Ma. Sample SE1F 1910 (n=215) age spectrum ranges from 352-2129 Ma; peak ages are 467, 533, and 1082 Ma. Sample SE1F 1911 (n=271) has age peaks of 465, 526 and 1094 Ma. Zircons range in age from 227 to 3412 Ma. The maximum depositional age for this succession based on the overlapping age of the youngest subset of zircons is 333.6±2.4 Ma. K-S analysis indicates that the lower two samples are statistically related (US1A 1902 and SE1A 1901); the second and third samples (SE1A 1901 and SE1D 1905) also are related. SE1F 1907 and SE1F 1910 are unrelated to any other sample. The uppermost sample SE1F 1911 is related to the Tupe and Guandacol formations in the Paganzo Basin, which in turn is related to the Itararé Formation in Brazil.

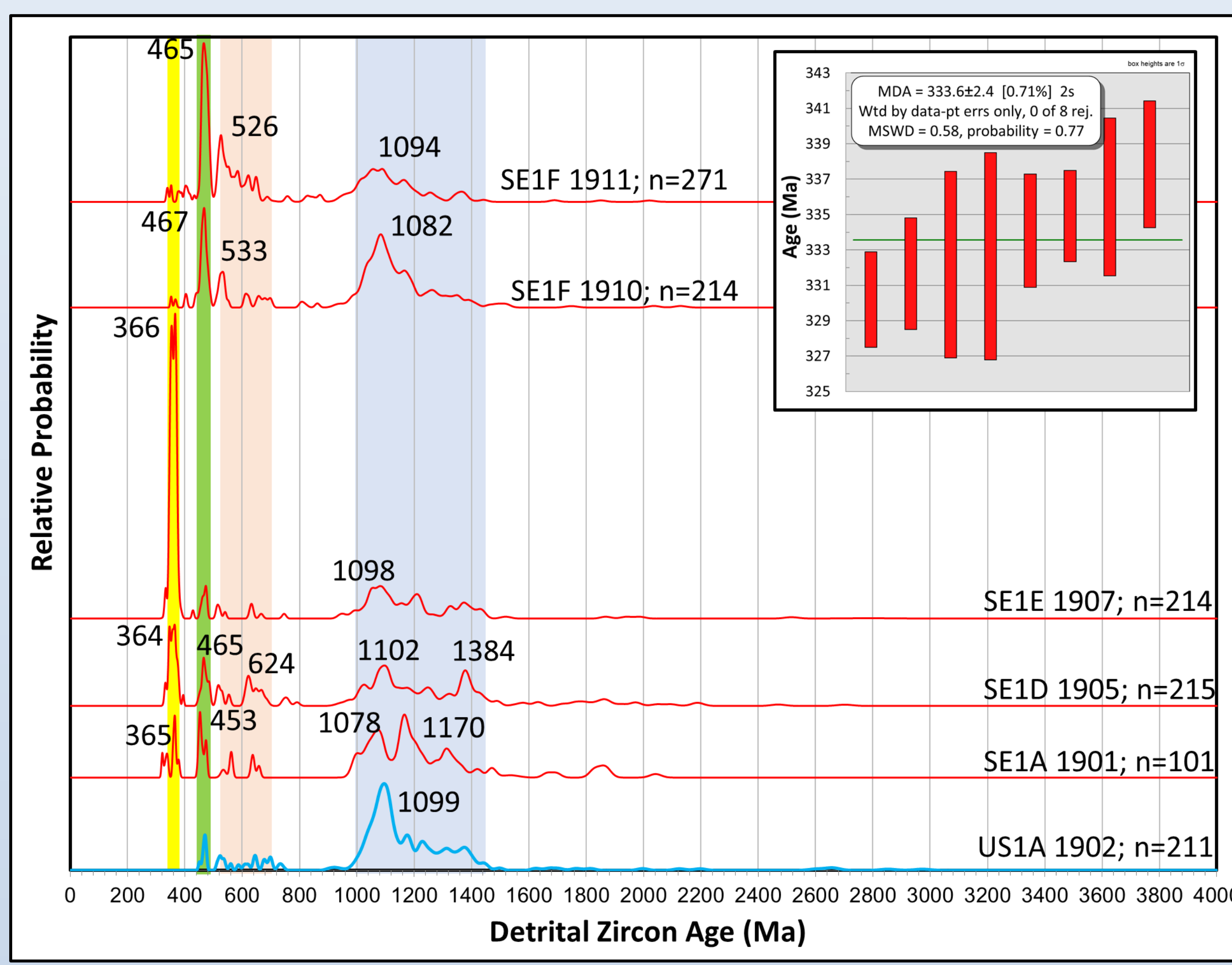


Figure 7. Stacked probability plots of samples analyzed as part of this project. The timing of Gondwanan orogenies are indicated by the colored backgrounds. Yellow = Chañi orogeny (~360-390 Ma), green = Famatinian orogeny (~450-490 Ma), pink = Pan-African orogeny (~520-700 Ma), and blue = Sunsas orogeny (1000-1450 Ma). Inset = maximum depositional age estimate.

	US1A 1902	SE1A 1901	SE1D 1905	SE1E 1907	SE1F 1910	SE1F 1911	Tupe	Guandacol	Loma Larga	Malanzán	Agua Colorado	Itararé São Fran.	Itararé Paraná	Sauce Grande
US1A 1902	0.000	0.229	0.000	0.000	0.001	0.000	0.000	0.000	0.000	0.000	0.000	0.000	0.000	0.000
SE1A 1901	0.229	0.054	0.000	0.004	0.000	0.000	0.000	0.000	0.000	0.000	0.000	0.000	0.001	0.000
SE1D 1905	0.000	0.054	0.000	0.003	0.003	0.000	0.000	0.000	0.000	0.000	0.000	0.001	0.001	0.003
SE1E 1907	0.000	0.000	0.000	0.000	0.000	0.000	0.000	0.000	0.000	0.000	0.000	0.000	0.000	0.002
SE1F 1910	0.001	0.004	0.003	0.000	0.000	0.000	0.000	0.000	0.000	0.000	0.000	0.000	0.000	0.000
SE1F 1911	0.000	0.000	0.000	0.000	0.000	0.000	0.381	0.469	0.000	0.000	0.000	0.103	0.000	0.000
Tupe	0.000	0.000	0.000	0.000	0.000	0.000	0.381	0.978	0.023	0.000	0.000	0.207	0.000	0.000
Guandacol	0.000	0.000	0.000	0.000	0.000	0.000	0.469	0.978	0.007	0.000	0.000	0.316	0.000	0.000
Loma Larga	0.000	0.000	0.000	0.000	0.000	0.000	0.023	0.007	0.032	0.000	0.000	0.001	0.000	0.000
Malanzán	0.000	0.000	0.000	0.000	0.000	0.000	0.000	0.000	0.032	0.000	0.296	0.000	0.000	0.000
Agua Colorado	0.000	0.000	0.000	0.000	0.000	0.000	0.000	0.000	0.000	0.000	0.296	0.000	0.000	0.000
Itararé São Fran.	0.000	0.000	0.001	0.000	0.000	0.000	0.103	0.207	0.001	0.000	0.000	0.128	0.067	0.000
Itararé Paraná	0.000	0.001	0.000	0.000	0.000	0.000	0.000	0.000	0.000	0.000	0.000	0.128	0.321	0.000
Sauce Grande	0.000	0.000	0.003	0.000	0.002	0.000	0.000	0.000	0.000	0.000	0.000	0.067	0.321	0.000

Table 1. K-S analysis of late Paleozoic glaciogenic strata in South America. Red = this study, orange = Paganzo basin, green = Itararé group in the Paraná and São Francisco basins, and grey = Sauce Grande formation in the Colorado Basin. Yellow-bold = P value of <math>0.05</math>, which indicates the age spectra are statistically not different and thus the samples may share the same provenance.

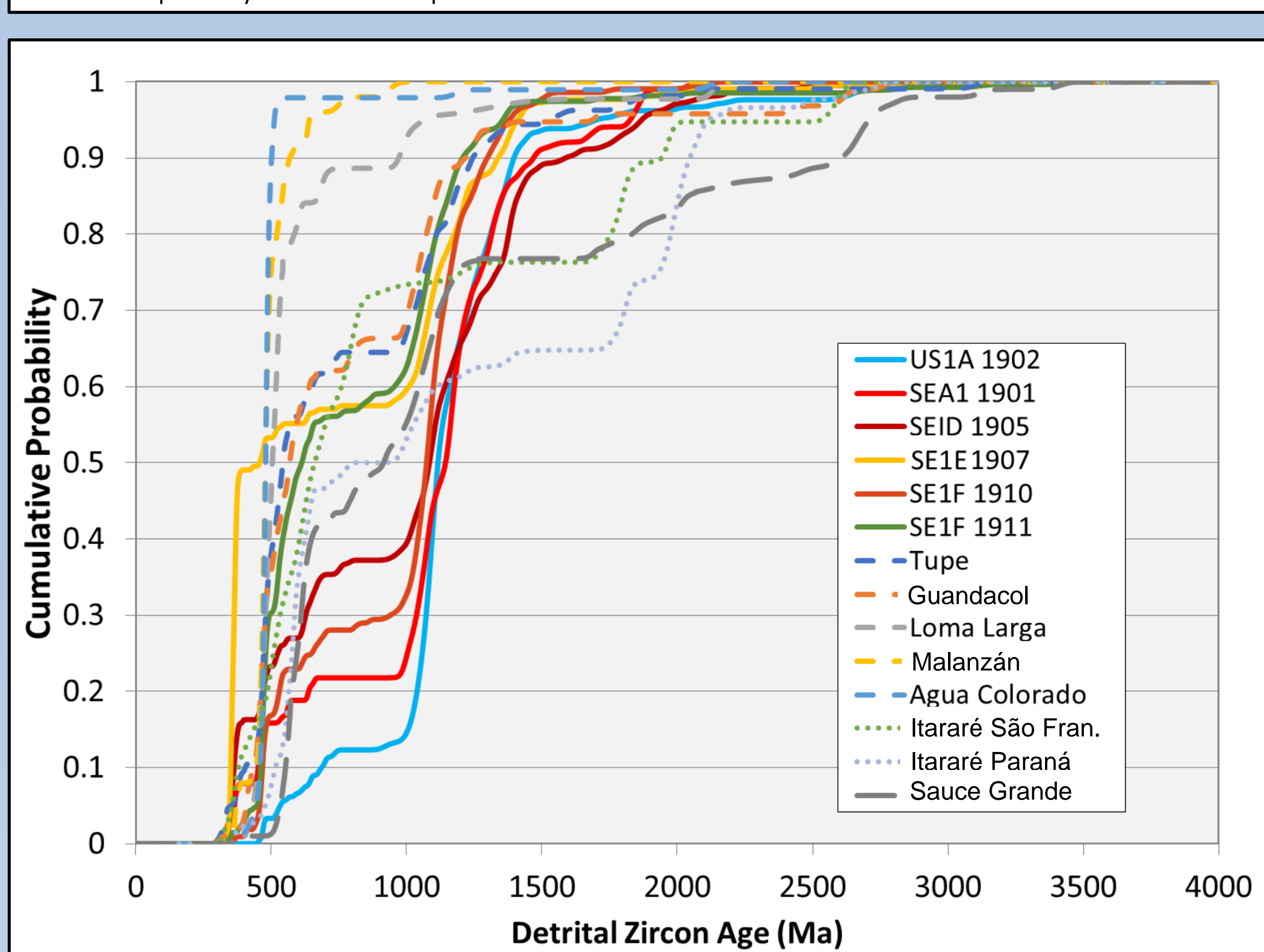


Figure 8. Detrital zircon age cumulative curves for the samples analyzed here (solid lines) as compared to Carboniferous glaciogenic strata in other South American basins provided in Craddock et al. (2019). The Tupe, Guandacol, Loma Larga, Malanzán and Agua Colorado (Paganzo basin, medium dash line), the Itararé Group in the Paraná Basin (dotted lines), and the Sauce Grande Formation (long dash line) in the Colorado Basin (equivalent to the Karoo Basin in South Africa).

**Discussion**  
For this study, depositional processes have been refined from previous work in order to incorporate new data taken from the field (López-Gamundi, 1987; Taboada, 2004). The lithofacies are dominated by marine processes, similar to those found in normal shelf and slope settings. These lithofacies include: suspension settling of hemipelagic sediments, wave and current activity, sediment gravity flows, as well as shallow marine and fluvial sands. While the occurrence of striated and faceted clasts are common in the lower 400m of the section, evidence for proximal glaciers/ice sheets is lacking (i.e. grooved pavements, roche moutonnées). López-Gamundi (1987) characterized the depositional model for the glaciomarine strata as a glacial drift build-up on a depositional slope, dominated by sediment gravity flows and turbidity currents. This interpretation conforms with our new findings, and our contribution includes the addition of a trough mouth fan deposit, emphasized by the delivery of large volumes of subglacial sediment to shelf-slope margin, and the subsequent re-deposition of this glaciogenic sediment down the continental slope via debris-flow processes.

The maximum depositional age for the San Eduardo Formation is 333.6±2.4 Ma, which indicates that it is broadly correlative with similar strata in the Paganzo basin and consisted being deposited in glacial stage 2 from Craddock et al. (2019). Underlying Silurian strata are dominated by sediment derived from basement rocks formed during the 1000-1450 Ma Sunsas orogeny. Samples with direct glacial influence (SE1A 1901, SE1D 1905, SE1E 1907) show a distinct population of young zircons related to the Chañi orogeny (~360-390 Ma). This Chañi peak becomes more prominent in the uppermost sample in this part of the section. The number of young grains increase with elevation while the Mesoproterozoic population decreases, suggesting a more proximal sediment source area or stages of unroofing. A small age peak at ~465 Ma exists in each of these samples as well, indicating that Famatinian rocks contributed some sediment to the San Eduardo formation. Samples SE1F 1910 and SE1F 1911 have much different detrital zircon age spectra than our lowermost samples. No Chañi signal is evident here and the ~465 Famatinian signal is the most dominant. Each of these samples also have prominent Pan-African (~530 Ma) and Sunsas (~1090 Ma). Sample SE1F 1911 also has the oldest zircons that we analyzed, including 2 that are >3000 Ma. These were most likely derived from the São Francisco craton, Brazil (Martin et al., 1997), which is consistent with the emergence of the Pan-African signal as rocks of this age occur in this region as well.

Our highest sample (SE1F 1911) has a K-S match with both the Tupe and Guandacol Formations in the Paganzo basin. This relationship suggests a spatial and temporal link between the San Eduardo and the Tupe and Guandacol formations. Moreover, the Tupe-Guandacol and uppermost San Eduardo have a detrital zircon age spectra that are similar to rocks of the Itararé Formation in the Paraná basin of Brazil, which also suggests a more distal sediment contribution.

Sediment derivation and transport was directly impacted by the presence of local alpine glaciers. During the height of glaciation, as indicated by the volume of coarse clastic rocks, sediment was derived locally and then transported by glacial meltwater before being deposited in a trough mouth marine environment. After local alpine glaciation ceased and ice no longer filled fjord-like valleys during the collapse of the proto-Precordillera, sediment was transported from distal source areas to the northeast in the São Francisco craton and then transported by large fluvial systems to littoral environments during transgression.

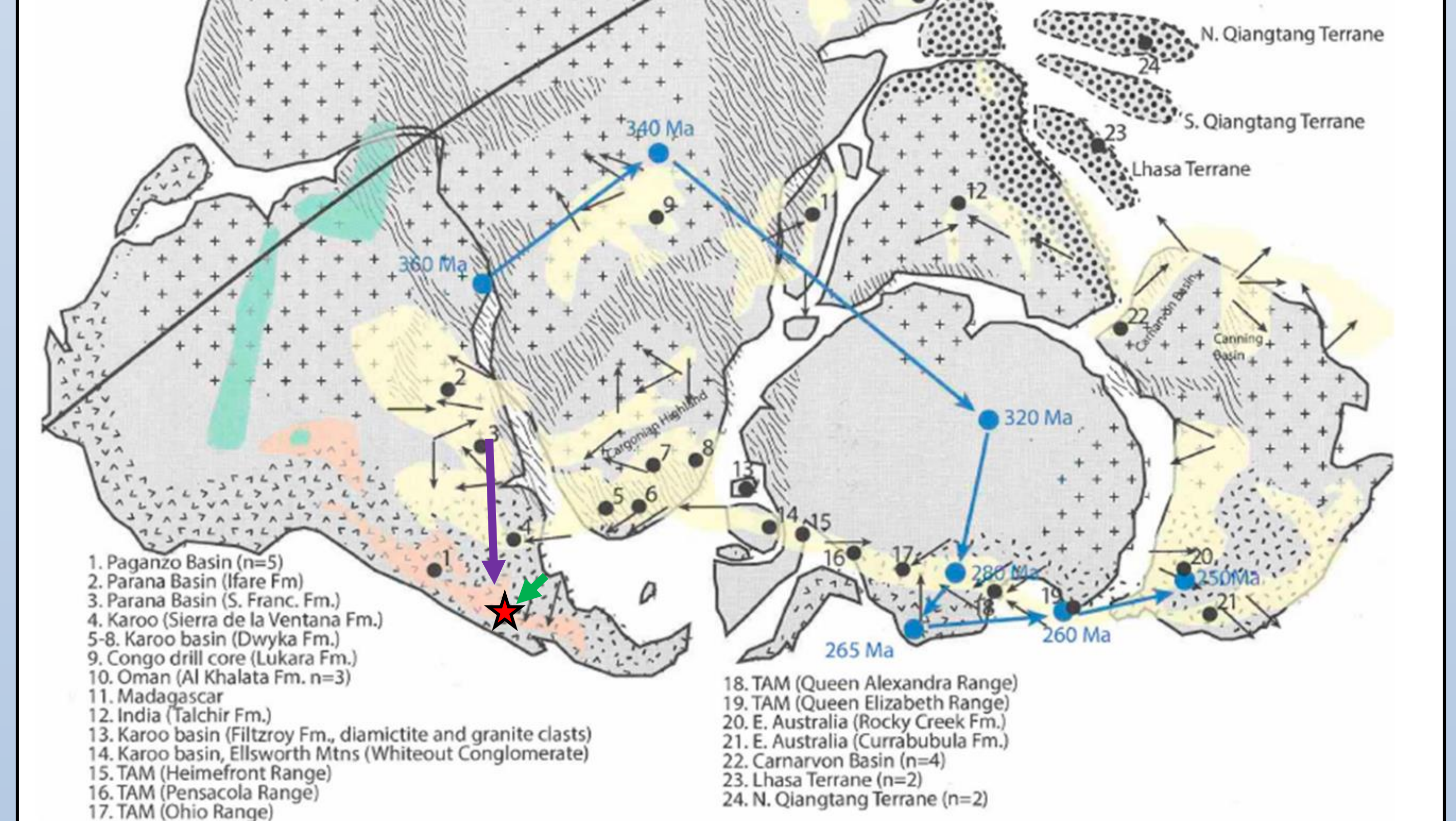


Figure 9. Gondwana during the late Paleozoic with schematic basement geology, the three episodes of LPIA glaciation indicated (Glacial Episode I: 360-342Ma; Glacial Episode II: 334-313Ma; Glacial Episode III: 315-265Ma) Modified from Craddock et al. (2019). Red star = our study area. Green arrow indicates locally sourced sediment deposited during alpine glaciation of the proto-Precordillera. Purple arrow indicates distally sourced sediment deposited after alpine glaciation in the Calingasta-Uspallata basin.

**REFERENCES**  
• Craddock, J.P., Ojakangas, R. W., Malone, D.H., Konstantinou, A., Mory, A., Bauer, W., Thomas, R.J., Craddock-Affinati, S., Pauls, K., Zimmerman, U., Botha, G., Rochas-Campos, A., Tohver, E., Riccomini, C., Martin, J., Redfern, J., Horstwood, M., Gehrels, G., 2019, Provenance of Permo-Carboniferous Glacial Diamicrites across Gondwana: Earth-Science Reviews, v. 192, p. 285-316  
• Gehrels, G.E., Valencia, V., Ruiz, J., 2008, Enhanced precision, accuracy, efficiency, and spatial resolution of U-Pb ages by laser ablation-multicollector-inductively coupled plasma-mass spectrometry: Geochemistry, Geophysics, Geosystems, v. 9, Q03017  
• Gehrels, G. and Pecha, M., 2014, Detrital zircon U-Pb geochronology and Hf isotope geochemistry of Paleozoic and Triassic passive margin strata of western North America: Geosphere, v. 10, p. 49-65.  
• Henry, L.C., Isbell, J.L., Limarino, C.O., McHenry, L.J., Fraiser, M.L., 2010, Mid-Carboniferous deglaciation of the protop - Precordillera, Argentina recorded in the Agua de Gulbrán paleoalvalley: Palaeogeography, Palaeoclimatology, Palaeoecology, 298(1-2), p. 112-129.  
• Isbell, J.L., Henry, L.C., Gulbranson, E.L., Limarino, C.O., Fraser, M.L., Koch, Z.L., Ciccioli, P.L., Dineen, A.A., 2012, Glacial paradoxes during the LPIA: evaluating the equilibrium line altitude as a control on glaciation: Earth-Science Reviews, v. 22, p. 1-19.  
• Limarino, C., Tripaldi, A., Marensi, S., and Fauqué, L., 2006, Tectonic, sealevel, and climatic controls on late Paleozoic sedimentation in the western basins of Argentina: Journal of South American Earth Sciences, v. 33, no. 3-4, p. 205-226.  
• López-Gamundi, O.R., 1987, Depositional models for the glaciomarine sequences of Andean Late Paleozoic basin of Argentina: Sedimentary Geology, 52:109-126.  
• Ludwig, K., 2008, Isoplot 3.6: Berkeley Geochronology Center Special Publication 4, p. 77.  
• Ramos, V.A., Jordan, T.E., Allmendinger, R.W., Kay, S.M., Cortes, J.M., and Palma, M.A., 1984, Chileña; an allochthonous terrane in the Paleozoic evolution of the Central Andes: Actas del Congreso Geológico Argentino, v. 2, p. 84-106.  
• Ramos, V.A., Jordan, T.E., Allmendinger, R.W., Mpodzois, M.C., Kay, S.M., Cortes, J.M., and Palma, M., 1986, Paleozoic terranes of the central Argentine-Chilean Andes: Tectonics, v. 5, p. 855-880.  
• Taboada, A. C., 2004, Braquiópodos y bioestratigrafía del Carbonífero del Córdon del Naranjo (Subcuenca Calingasta-Uspallata), Argentina: Ameghiniana, 41(3), p.405-422.